Real-Time Load Elasticity Tracking and Pricing for Electric Vehicle Charging

Nasim Yahya Soltani, *Student Member, IEEE*, Seung-Jun Kim, *Senior Member, IEEE*, and Georgios B. Giannakis, *Fellow, IEEE*

***Abstract*—While electric vehicles (EVs) are expected to provide environmental and economical benefit, judicious coordination of EV charging is necessary to prevent overloading of the distribution grid. Leveraging the smart grid infrastructure, the utility company can adjust the electricity price intelligently for individual customers to elicit desirable load curves. In this context, this paper addresses the problem of predicting the EV charging behavior of the consumers at different prices, which is a prerequisite for optimal price adjustment. The dependencies on price responsiveness among consumers are captured by a conditional random field (CRF) model. To account for temporal dynamics potentially in a strategic setting, the framework of online convex optimization is adopted to develop an efficient online algorithm for tracking the CRF parameters. The proposed model is then used as an input to a stochastic profit maximization module for real-time price setting. Numerical tests using simulated and semi-real data verify the effectiveness of the proposed approach.**

***Index Terms*—Conditional random field (CRF), online convex optimization, real-time pricing, smart grid.**

NOMENCLATURE

E	Set of edges (dependency) in graph G.
G	Graph of spatial dependency of consumer behaviors.
M	Total number of consumers.
V	Set of nodes (consumers) in graph G.
b_i^t	EV charging decision of consumer i at time t.
P_{EV}	Charging power flow.
$P_{\max}$	Aggregate load power threshold.
α, β, γ	Coefficients for generation cost function.
$\mathcal{D}_i$	Charging deadline of consumer i.
$\mathcal{E}_i$	Total charging capacity of consumer i.
η_i^t	Nonelastic load of consumer i at time t.
ℓ^t	Loss function.
ϕ_i	Feature function capturing dependency of charging decision of consumer i on the price ρ_i^t.
$\psi_{i,j}$	Feature function capturing dependency of charging decisions between consumers i and j.
ρ_i^t	Price for consumer i at time t.
$\mathbf{\Sigma}^t$	Covariance matrix encoding the dependency graph.
τ_i^t	Charging decision threshold.
$\tilde{\mathcal{D}}_i^t$	Time left to the deadline for EV i at time t.
$\tilde{\mathcal{E}}_i^t$	Charging energy needed for EV i at time t.
$\theta_{i,j}^t$	CRF model parameter capturing dependency between consumers i and j at time t.
θ_i^t	CRF model parameter capturing price dependency of consumer i at time t.
ζ	Elasticity coefficient.

Manuscript received April 22, 2014; revised August 27, 2014; accepted October 11, 2014. This work was supported in part by the National Science Foundation (NSF)-Computing and Communication Foundations (CCF) under Grant 1423316, Grant CyberSEES 1442686, and NSF Grant 1202135, and in part by the Institute of Renewable Energy and the Environment under Grant RL-0010-13. A part of this work was presented at the Computational Advances in Multi-Sensor Adaptive Processing (CAMSAP) Conference, Saint Martin, Dec. 15–18, 2013. Paper no. TSG-00339-2014.

N. Y. Soltani and G. B. Giannakis are with the Department of Electrical and Computer Engineering, University of Minnesota, Minneapolis, MN 55455 USA (e-mail: yahya015@umn.edu; georgios@unm.edu).

S.-J. Kim is with the Department of Computer Science and Electrical Engineering, University of Maryland, Baltimore County, Baltimore, MD 21250 USA (e-mail: sjkim@umbc.edu).

Color versions of one or more of the figures in this paper are available online at http://ieeexplore.ieee.org.

Digital Object Identifier 10.1109/TSG.2014.2363837

I. INTRODUCTION

THE SMART grid vision aims at capitalizing on information technology for efficient use of energy resources in grid operation with reliability assurance and consumer participation. Recently, there has been a growing interest in incorporating electric vehicles (EVs), which are expected to be widely deployed in the near future [1]. EV penetration may contribute to alleviating dependence on fossil fuel and cutting greenhouse gas emissions. EV owners may also benefit from lower energy cost in the face of spiking gasoline prices.

Although environmental and economical benefit due to transportation electrification may be huge, simultaneous charging of a large number of EVs in residential distribution grids can significantly overload the infrastructure. Uncoordinated EV charging can aggravate load peaks owing to concentrated charging demand before commuting hours, resulting in higher cost for grid operation [2]–[4]. Therefore, coordinated charging of EVs is a crucial task for future power systems.

In order to elicit desirable electricity consumption patterns, various time-based pricing schemes have been proposed. By allowing the electricity price to vary over different hours of a day, consumers are encouraged to shift inessential loads to the periods of low prices, which generally correspond to off-peak hours [5]. There is an extensive literature on scheduling the time and rate of EV charging [6]–[13]. The generation and EV charging costs were minimized in [7] under power-flow constraints. With the goal of shifting EV loads to fill the overnight demand valley, a distributed algorithm for day-ahead charging rate schedules was proposed in [8]. The EV charging schedule was optimized by minimizing load variance

and maximizing load factor in [9]. A real-time distributed algorithm was proposed to shift the elastic loads to the periods of high renewable generation [10].

Prerequisite to the demand coordination task is to obtain reliable analytics. In addition to the essential load and price forecasting tasks, it is instrumental also to learn the consumers' behavioral patterns. In [14], smart grid consumers' price elasticity was estimated using a linear regression model with price changes as regressors and the corresponding shift in total demand as the response. The price responsiveness is useful, for instance, when one desires to set the prices optimally with various objectives such as minimizing the generation cost or maximizing the net profit from grid operation.

However, existing techniques for acquiring price elasticity fall short of capturing some important aspects. First, in practice, price elasticity might change over time even in an adversarial and strategic manner, as the consumers can react to price changes to maximize their own profit. Thus, accounting for the dynamics of consumer preferences is critical. Secondly, the spatial dependencies of consumer behaviors, e.g., the correlations existent in the behaviors of consumers, which may be due to similar lifestyles of the people in geographic proximity with comparable income levels, or even due to technical/strategic reasons involving overloaded distribution networks [15], have not been exploited. Furthermore, in terms of algorithm implementation, online algorithms are preferred over batch alternatives for real-time processing of streaming data.

This paper adopts a statistical model that captures the dependency of EV consumers' charging decisions on the announced electricity price. As the charging decisions can be best described by discrete values (e.g., "charging" or "not charging"), a logistic regression-type framework is employed. To capture spatial dependence of the behaviors, the dependency structure is modeled as a graph, and the overall model corresponds to a conditional random field (CRF) [16]. An online algorithm is then developed to track the relevant model parameters, based on an online learning framework [17], which provides performance guarantees with minimal assumptions on the structure of temporal dynamics.

Compared to other alternatives such as fully generative Bayesian approaches and nonparametric kernel models, the CRF framework is appealing as the EV charging behavior is discrete, which invites logistic regression-type approaches. Furthermore, compared to the fully generative Bayesian models, the CRF approach is widely appreciated due to its merit of not requiring a statistical model for the control variables, which in our case is the price vector [18]. Finally, the CRF framework naturally accommodates risk-limiting stochastic optimization formulations for price setting.

Some prior works captured the strategic interdependency of the consumers through a game theoretic framework [6], [19]–[21]. A noncooperative Stackelberg game model was adopted in [19], where the utility sets the price to optimize its revenue and the EV charging customers optimize their charging strategies. A mechanism to encourage the EVs to participate in frequency regulation was introduced in a vehicle-to-grid scenario in [20]. The stored energy in the EV batteries was traded in a noncooperative game setup in [21], where the prices were determined via an auction mechanism. Since statistical models, whose parameters are adapted over time, are employed in this paper, our approach is fairly general, and can potentially apply to a broad range of practical scenarios.

The proposed algorithm yields the consumers' EV charging probability distribution, conditioned on the announced electricity prices, which is a prerequisite for stochastic economic dispatch or profit maximization formulations. Existing works on stochastic profit maximization accounting for load elasticity and uncertainty under real-time pricing include [22] and [23]. A demand elasticity model is postulated in [22] to maximize total income (the area under a price-demand curve) and minimize generation costs. However, the parameters of the load elasticity model are assumed known and fixed over time and the dependencies among consumers are neglected. The real-time pricing approach in [23] again entails maximization of a certain utility function minus cost. However, load uncertainty was captured through a simplistic model involving a typical load perturbed by a random variable. In contrast, this paper properly captures spatio-temporal dependency and variability of consumers' price responsiveness, learns them in an online fashion, and exploits them for real-time price setting with a pertinent goal of stochastic profit maximization.

Since our proposed approach is a closed-loop strategy that adjusts the prices in response to consumer behaviors, a real data set cannot be easily obtained. To test the efficacy of the proposed approaches, both synthetic and semi-real data sets were utilized, where in the latter case, a reasonable consumer behavior model was fitted to available real data to simulate price-dependent consumer behavior.

Compared to our conference precursor [24], a number of new contributions are made in this paper. First, while only the online estimation of consumer behavior depending on prices was considered in [24], here a stochastic revenue optimization formulation is proposed for real-time price setting based on the predictions, closing the loop. Secondly, while the conference work tested the CRF parameter estimation using only synthetic data, this paper employed semi-real data as well to validate the entire algorithm including the price setting part in a more realistic setup.

The rest of this paper is organized as follows. Section II states the problem and recaps the CRF modeling framework. Section III develops an online algorithm for estimating the model parameters. In Section IV, the real-time price setting problem is formulated. Results of numerical tests are presented in Section V, and the conclusion is provided in Section VI.

II. Problem Statement

A. System Model

The goal of a load serving entity is to shape the EV charging load imposed to the distribution grid in some desirable way, so as to minimize the generation cost, or maximize the net profit. One way of achieving this is to set the electricity prices for individual consumers appropriately in order to influence the

consumers' EV charging behavior. For this, it is first necessary to estimate how responsive individual consumers are at each time to different prices presented to them.

Consider M EV owners, who desire to charge their EVs via a distribution network. Let $b_i^t \in \mathcal{S} := \{0, 1\}$ indicate the charging behavior of consumer i at time t; i.e., $b_i^t = 1$ when consumer i is charging his EV at time t, and $b_i^t = 0$, otherwise.[1] Similarly, ρ_i^t denotes the electricity price during time slot t for consumer i.[2] To capture spatial dependence (e.g., behavioral dependence of consumers living in the same neighborhood, or having similar income levels), an undirected graph $G = (V, E)$ is introduced, where the vertex set $V := \{1, 2, \ldots, M\}$ corresponds to the consumers, and edges $(i, j) \in E$ capture the dependence between consumers i and j. Since the edges are undirected, it is assumed that $(i, j) \in E$ if $(j, i) \in E$.

It is assumed that the customer premises are equipped with smart meters so that bi-directional communication between the utility and the consumers is feasible. Leveraging such an advanced metering infrastructure, the utility announces prices $\{\rho_i^t\}$ to all consumers $i \in V$ at the beginning of slot $t = 1, 2, \ldots$. Subsequently, the charging decisions $\{b_i^t\}$ of the consumers are reported back to the utility at the end of slot t.

In this context, the following problem is of interest: estimate the probability with which each consumer $i \in V$ will charge the EV at time t paying for price $\{\rho_i^t\}$, given past prices $\{\rho_i^\tau, i \in V, \tau = 1, \ldots, t-1\}$, and the corresponding observed charging behaviors $\{b_i^\tau, i \in V, \tau = 1, \ldots, t-1\}$, while accounting for possible spatial dependencies in $\{b_i^t\}$ captured by G.

B. CRF Model for EV Charging Behavior

To solve the aforementioned problem, the framework of CRFs is adopted [16]. Collect in vectors $\mathbf{b}^t$ and $\boldsymbol{\rho}^t$ variables $\{b_i^t\}_{i=1}^M$ and $\{\rho_i^t\}_{i=1}^M$, respectively. The CRF models the conditional probability distribution function (pdf) $p(\mathbf{b}^t|\boldsymbol{\rho}^t)$. In short, $p(\mathbf{b}^t|\boldsymbol{\rho}^t)$ is a CRF with respect to G if it obeys the Markov property for every $\boldsymbol{\rho}^t$. This means that conditioned on $\boldsymbol{\rho}^t$, for any node pair $(i, j) \in V$, behavior b_i^t is independent of b_j^t given the neighbors $b_k^t \in N(i) := \{k{:}(i, k) \in E\}$. Intuitively, this means that given $\boldsymbol{\rho}^t$, the behavior of the neighbors of b_i^t contains all the information needed for predicting b_i^t, and other variables are irrelevant.

Let $\psi_{i,j}(b_i^t, b_j^t)$ denote the feature functions quantifying the dependency in charging behavior of consumers i and j. In addition, functions $\phi_i(b_i^t, \rho_i^t)$ model the dependency of b_i^t on price ρ_i^t. Parameters θ_i^t and $\theta_{i,j}^t$ are introduced for ϕ_i and $\psi_{i,j}$, respectively, to capture the strengths of these dependencies. With $\boldsymbol{\theta}^t := [\theta_i^t, i \in V; \theta_{i,j}^t, (i, j) \in E]$, the price-conditional behavior pdf can be modeled as

$$p_{\boldsymbol{\theta}^t}\left(\mathbf{b}^t|\boldsymbol{\rho}^t\right) = \frac{1}{Z(\boldsymbol{\rho}^t)} \prod_{i \in V} e^{\theta_i^t \phi_i(b_i^t, \rho_i^t)} \prod_{(i,j) \in E} e^{\theta_{i,j}^t \psi_{i,j}\left(b_i^t, b_j^t\right)} \quad \text{(1a)}$$

$$Z(\boldsymbol{\rho}^t) := \sum_{\mathbf{b}^t \in \mathcal{S}^M} \prod_{i \in V} e^{\theta_i^t \phi_i(b_i^t, \rho_i^t)} \prod_{(i,j) \in E} e^{\theta_{i,j}^t \psi_{i,j}\left(b_i^t, b_j^t\right)} \quad \text{(1b)}$$

where $Z(\boldsymbol{\rho}^t)$ is a normalization factor, also known as the partition function. Motivated by the CRF model pdf involved with logistic regression, we adopt the function

$$\phi_i\left(b_i^t, \rho_i^t\right) := b_i^t \rho_i^t. \quad (2)$$

Furthermore, inspired by the Ising model for modeling dependencies of binary random variables [25]

$$\psi_{i,j}\left(b_i^t, b_j^t\right) := b_i^t b_j^t \quad (3)$$

is chosen. Now the problem of finding $p_{\boldsymbol{\theta}^t}(\mathbf{b}^t|\boldsymbol{\rho}^t)$ given $\{\rho_i^\tau, b_i^\tau, i \in V, \tau = 1, \ldots, t-1\}$ translates to estimating $\boldsymbol{\theta}^t$ at each time t.

III. Online Learning of Load Elasticity

Compared to batch algorithms that process the entire collection of data to obtain the desired estimates, online algorithms feature the capability to process data one-by-one in a sequential fashion. To develop an online algorithm for estimating $\boldsymbol{\theta}^t$, the approach here utilizes online convex optimization, which requires minimal assumptions on the temporal dynamics of $\boldsymbol{\theta}^t$, and can provide provable performance guarantees even in adversarial settings [17], [26], [27]. Such guarantees against adversarial players are meaningful because the consumers may act strategically to maximize their own benefit (and mend their price responsiveness accordingly). Next, the online convex programming framework is outlined.

A. Online Convex Programming

Online convex programming can be viewed as a multiround game with a forecaster and an adversary. The loss functions $\ell^t(\cdot)$ associated with the forecasts for $t = 1, 2, \ldots, T$, and the feasible set $\boldsymbol{\Theta}$ are assumed convex. In round t, the forecaster chooses $\hat{\boldsymbol{\theta}}^t \in \boldsymbol{\Theta}$, after which the adversary reveals $\ell^t(\cdot)$, incurring loss $\ell^t(\hat{\boldsymbol{\theta}}^t)$ for the tth round. Performance of the online actions $\{\hat{\boldsymbol{\theta}}^t\}$ is assessed through the so-termed regret given by

$$R_T = \sum_{t=1}^{T} \ell^t\left(\hat{\boldsymbol{\theta}}^t\right) - \min_{\boldsymbol{\theta} \in \boldsymbol{\Theta}} \sum_{t=1}^{T} \ell^t(\boldsymbol{\theta}) \quad (4)$$

which represents the relative cumulative loss of the online forecaster after T rounds, compared to an optimal offline minimizer, which has the advantage of hindsight. Online convex programming algorithms provide ways to generate the sequence $\{\hat{\boldsymbol{\theta}}^t\}_{t=1}^T$ to achieve a regret that is sublinear in T.

[1] Multiple charging rates can be accommodated straightforwardly by increasing the number of labels in $\mathcal{S}$.

[2] The price adjustment in this paper models the incentives given to the individual customers in various forms, and may correspond to actual rate charged if the customers sign up with such an arrangement. The economic benefit that the utility receive through such incentivization scheme can eventually be distributed to the consumers. Our scheme allows performing heavier incentivization for the consumers who are more sensitive to it, thus rewarding such consumers more. On the other hand, it is emphasized that the price setting can be done while accommodating any regulatory and socio-ethical constraints; see Remark in Section IV.

TABLE I
BELIEF PROPAGATION ALGORITHM FOR COMPUTING $\{p(b_i^t|\boldsymbol{\rho}^t)\}$ AND $\{p(b_i^t, b_j^t|\boldsymbol{\rho}^t)\}$

1: Initialize $m_{ij}^{(0)}(b_j^t) = 1$ for all $i, j \in V$ and $b_j^t \in \mathcal{S}$.
2: For $n = 1, 2, ...,$ MAX_ITER
Perform for all $i, j \in V$ and $b_j^t \in \mathcal{S}$:
3: Update: $m_{ij}^{(n)}(b_j^t) \leftarrow \sum_{b_i^t \in \mathcal{S}} \exp\left(\theta_i^t \phi_i(b_i^t, \rho_i^t)\right) \exp\left(\theta_{i,j}^t \psi_{i,j}(b_i^t, b_j^t)\right) \prod_{\nu \in N(i)\setminus\{j\}} m_{\nu i}^{(n-1)}(b_i^t)$
4: Normalize: $m_{ij}^{(n)}(b_j^t) \leftarrow \zeta_1^{-1} m_{ij}^{(n)}(b_j^t)$, where $\zeta_1 := \sum_{b_j^t \in \mathcal{S}} m_{ij}^{(n)}(b_j^t)$
5: Next n
6: Set $m_{ij}(b_j^t) = m_{ij}^{(\text{MAX\_ITER})}(b_j^t)$ for all $i, j \in V$ and $b_j^t \in \mathcal{S}$.
7: Compute beliefs:
$\tilde{p}(b_i^t|\boldsymbol{\rho}^t) = \exp\left(\theta_i^t \phi_i(b_i^t, \rho_i^t)\right) \prod_{j \in N(i)} m_{ji}(b_i^t)$
$\tilde{p}(b_i^t, b_j^t|\boldsymbol{\rho}^t) = \exp\left(\theta_i^t \phi_i(b_i^t, \rho_i^t)\right) \exp\left(\theta_j^t \phi_j(b_j^t, \rho_j^t)\right) \exp\left(\theta_{i,j}^t \psi_{i,j}(b_i^t, b_j^t)\right) \prod_{\nu \in N(j)\setminus\{i\}} m_{\nu j}(b_j^t) \prod_{o \in N(i)\setminus\{j\}} m_{oi}(b_i^t)$
8: Normalize:
$p(b_i^t|\boldsymbol{\rho}^t) = \zeta_2^{-1} \tilde{p}(b_i^t|\boldsymbol{\rho}^t)$, where $\zeta_2 := \sum_{b_i^t \in \mathcal{S}} \tilde{p}(b_i^t|\boldsymbol{\rho}^t)$
$p(b_i^t, b_j^t|\boldsymbol{\rho}^t) = \zeta_3^{-1} \tilde{p}(b_i^t, b_j^t|\boldsymbol{\rho}^t)$, where $\zeta_3 := \frac{\sum_{b_i^t \in \mathcal{S}} \tilde{p}(b_i^t, b_j^t|\boldsymbol{\rho}^t)}{p(b_j^t|\boldsymbol{\rho}^t)}$

B. Online Learning of Load Elasticity

In our context, the forecaster is the utility company and the adversaries are the EV owners. The loss is represented by the negative log-likelihood function for maximum likelihood estimation of $\boldsymbol{\theta}^t$ [16], [28] as

$$\ell^t\left(\boldsymbol{\theta}^t\right) := -\log p_{\boldsymbol{\theta}^t}\left(\mathbf{b}^t\middle|\boldsymbol{\rho}^t\right) \tag{5}$$

which is not revealed to the utility company until the utility predicts $\hat{\boldsymbol{\theta}}^t$ and announces $\boldsymbol{\rho}^t$ based on $\hat{\boldsymbol{\theta}}^t$, since only then can the consumers respond with their charging decisions $\mathbf{b}^t$.

Note that the chosen loss $\ell^t(\boldsymbol{\theta}^t)$ in (5) with $p_{\boldsymbol{\theta}^t}(\mathbf{b}^t|\boldsymbol{\rho}^t)$ as in (1a) is convex [29]. A popular online convex programming algorithm relies on the online mirror descent (OMD) iteration, which is a projected subgradient method with the Bregman divergence used as a proximal term. It yields an efficient first-order algorithm with sublinear convergence rate [30]. Vector $\hat{\boldsymbol{\theta}}^{t+1}$ is obtained recursively in OMD as

$$\hat{\boldsymbol{\theta}}^{t+1} = \arg\min_{\boldsymbol{\theta}} \left\langle \nabla \ell^t\left(\hat{\boldsymbol{\theta}}^t\right), \boldsymbol{\theta} \right\rangle + \frac{1}{\mu^t} D\left(\hat{\boldsymbol{\theta}}^t \middle\| \boldsymbol{\theta}\right) \tag{6}$$

where μ^t denotes a step size, and $D(\cdot\|\cdot)$ represents the Bregman divergence. The Bregman divergence associated with the ℓ_2-norm is simply given by $D(\hat{\boldsymbol{\theta}}^t\|\boldsymbol{\theta}) = 1/2\|\boldsymbol{\theta} - \hat{\boldsymbol{\theta}}^t\|^2$. Upon substituting this into (6), the OMD update boils down to an online gradient descent given by

$$\hat{\boldsymbol{\theta}}^{t+1} = \hat{\boldsymbol{\theta}}^t - \mu^t \nabla \ell^t\left(\hat{\boldsymbol{\theta}}^t\right). \tag{7}$$

To evaluate the gradient in (7), for the likelihood in (5) and the pdf in (1a), it is shown in the Appendix that

$$\frac{\partial \ell^t}{\partial \theta_i^t} = \mathbb{E}\left\{b_i^t \rho_i^t \middle| \boldsymbol{\rho}^t\right\} - b_i^t \rho_i^t, \qquad \forall i \in V \tag{8}$$

$$\frac{\partial \ell^t}{\partial \theta_{i,j}^t} = \mathbb{E}\left\{b_i^t b_j^t \middle| \boldsymbol{\rho}^t\right\} - b_i^t b_j^t, \qquad \forall (i,j) \in E \tag{9}$$

where the expectation is with respect to $p_{\hat{\boldsymbol{\theta}}^t}(\mathbf{b}^t|\boldsymbol{\rho}^t)$.

Since b_i^t is a Bernoulli variable, it follows that:

$$\mathbb{E}\left\{b_i^t \rho_i^t \middle| \boldsymbol{\rho}^t\right\} = \rho_i^t p_{\hat{\boldsymbol{\theta}}^t}\left(b_i^t = 1 \middle| \boldsymbol{\rho}^t\right) \tag{10}$$

$$\mathbb{E}\left\{b_i^t b_j^t \middle| \boldsymbol{\rho}^t\right\} = p_{\hat{\boldsymbol{\theta}}^t}\left(b_i^t = 1, b_j^t = 1 \middle| \boldsymbol{\rho}^t\right). \tag{11}$$

TABLE II
OVERALL ONLINE ALGORITHM

1: Initialize $\hat{\boldsymbol{\theta}}^1$
2: For $t = 1, 2, \ldots$ do
3: Set prices $\boldsymbol{\rho}^t$ based on $\hat{\boldsymbol{\theta}}^t$.
4: Collect EV charging decisions $\mathbf{b}^t$.
5: Compute $\nabla \ell^t(\hat{\boldsymbol{\theta}}^t)$ using BP.
6: Update $\hat{\boldsymbol{\theta}}^{t+1} = \hat{\boldsymbol{\theta}}^t - \mu_t \nabla \ell^t(\hat{\boldsymbol{\theta}}^t)$
7: Next t

These marginal conditional probabilities can be efficiently evaluated by employing the belief propagation (BP) algorithm [31]. Starting with some initial messages, the BP algorithm performs message passing between nodes. The messages are updated iteratively until convergence or for a fixed number of iterations. The obtained messages can then be used for computing exact marginal probabilities for tree structured graphs. In graphs with loops, one needs to resort to the loopy belief propagation (LBP) algorithm [31], which often yields good approximations of marginals.

Let $m_{ij}(b_i^t)$ denote the message passed from node i to node j for $(i, j) \in E$. Then, based on the standard BP update rules, the updated messages $m_{ij}(b_j^t)$ and the marginals $p(b_i^t|\boldsymbol{\rho}^t)$ and $p(b_i^t, b_j^t|\boldsymbol{\rho}^t)$ are obtained as summarized in Table I [31]. The main computational burden of the BP algorithm lies in the message update step, which is $\mathcal{O}(|\mathcal{S}|^2)$ for each pair of nodes. This is considerably better than the $\mathcal{O}(|\mathcal{S}|^M)$ complexity incurred by computing marginals through direct summation over all variables.

The overall online algorithm for estimating $\boldsymbol{\theta}^{t+1}$ is summarized in Table II. Steps 5 and 6 confirm that $\hat{\boldsymbol{\theta}}^{t+1}$ is dependent on past values of $\{\boldsymbol{\theta}^\tau\}_{\tau=1}^t$, and thus on $\{\mathbf{b}^\tau, \boldsymbol{\rho}^\tau\}_{\tau=1}^t$ as well. Therefore, (7) makes use of the information in the entire input history. An instance of price setting algorithm for step 3 will be discussed in Section IV.

Clearly, consumers' charging decisions are correlated across time in practice. Compared to stochastic approximation alternatives [32], the novel algorithm based on online convex programming requires minimal assumptions on the structure of temporal correlation of data (charging decisions). In addition, the framework accommodates strategic actions of the consumers [17].

C. Performance Analysis

The algorithm in Table II yields a regret bound that is sublinear in T, as described in the following proposition.

Proposition 1: Let $N_e := |E|$ denote the number of edges in E. If $\max\{|\theta_i^t|, |\theta_{i,j}^t|\} \leq \theta_0$ and $|\rho_i^t| \leq \rho_0$ for all t, $i \in V$, and $(i,j) \in E$, then for $\{\hat{\boldsymbol{\theta}}^t\}$ obtained from the algorithm in Table II, it holds that

$$R_T \leq \theta_0 \sqrt{2\left(M\rho_0^2 + N_e\right)T} = O\left(\sqrt{T}\right). \tag{12}$$

Proof: See the Appendix. ■

Regarding practicality of the assumptions, it is natural to assume that the prices are bounded. In addition, to account for consumers that do not respond to price changes (corresponding to $\theta_i^t = \pm\infty$), one can use a sufficiently large bound for $\max\{|\theta_i^t|, |\theta_{i,j}^t|\}$ in practice. Thus, the conditions in Proposition 1 can be readily satisfied.

D. Dynamic Logistic Regression Benchmark

If one neglects the spatial dependencies by setting $\theta_{i,j} = 0$ for $(i,j) \in E$, the CRF model reduces to M parallel logistic regression models; that is [see (1a)]

$$p_{\boldsymbol{\theta}^t}\left(\mathbf{b}^t|\boldsymbol{\rho}^t\right) = \frac{1}{Z(\boldsymbol{\rho}^t)} \exp\left(\sum_{i\in V} \theta_i^t b_i^t \rho_i^t\right) = \prod_{i=1}^{M} \frac{e^{\theta_i^t b_i^t \rho_i^t}}{1 + e^{\theta_i^t \rho_i^t}}. \tag{13}$$

To obtain online estimates of $\{\theta_i^t\}$, the algorithm in Table II is again applicable, but the gradient evaluation can be performed without using BP, simply as

$$\frac{\partial \ell^t}{\partial \theta_i^t} = \frac{\rho_i^t e^{\theta_i^t \rho_i^t}}{1 + e^{\theta_i^t \rho_i^t}} - b_i^t \rho_i^t, \qquad i \in V. \tag{14}$$

IV. CRF-Based Real-Time Price Setting

So far, we have developed models and algorithms to capture consumers' EV charging decisions. Since the CRF model provides the probability distribution of the charging decisions given the prices, one can now formulate a risk-limiting stochastic optimization problem to tailor the EV charging demand in some desirable fashion. Here, a price setting formulation for maximizing the utility's net profit is considered, where the profit equals the revenue collected from customers minus power generation cost.

The idea is that through the learned CRF model, the utility can predict the overall load and the corresponding income as well as the generation cost accurately at each time t for arbitrary price vector $\boldsymbol{\rho}^t$. On the other hand, the utility must make sure that various operational constraints, such as the capacity constraints, are met all times. Thus, the relevant optimization problem maximizes the net profit while the risk of the total demand exceeding a certain limit is constrained to be low. Since the risk constraint is not easily expressed in closed form, a Gaussian approximation is employed to obtain a tractable formulation.

Let P_{EV} denote the charging rate for a single EV, and η_i^t represent the aggregate base load of household i at time t. Then

$$d_{\text{tot}}^t := \textstyle\sum_{i=1}^{M} \left(P_{\text{EV}} b_i^t + \eta_i^t\right) \quad u_{\text{tot}}^t := \textstyle\sum_{i=1}^{M} \rho_i^t \left(P_{\text{EV}} b_i^t + \eta_i^t\right) \tag{15}$$

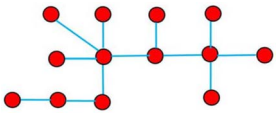

Fig. 1. Spatial dependency graph for the simulated test.

correspond to the total demand and payment due to M consumers at time t, respectively.

The generation cost is modeled as quadratic in total power P as $\alpha P^2 + \beta P + \gamma$, where α, β and γ are constants. Then, the problem of interest is to maximize the expected net profit while the chance of the total load exceeding certain threshold is smaller than a specified risk level. Formally, this corresponds to

$$\text{(P1)} \quad \max_{\mathbf{0} \preceq \boldsymbol{\rho}^t \preceq \bar{\boldsymbol{\rho}}} \mathbb{E}\left\{u_{\text{tot}}^t - \left[\alpha\left(d_{\text{tot}}^t\right)^2 + \beta d_{\text{tot}}^t + \gamma\right] \middle| \boldsymbol{\rho}^t\right\} \tag{16a}$$

$$\text{subject to } \Pr\left\{d_{\text{tot}}^t > P_{\max} | \boldsymbol{\rho}^t\right\} \leq \epsilon \tag{16b}$$

where the expectation is with respect to $p_{\hat{\boldsymbol{\theta}}^t}(\mathbf{b}^t|\boldsymbol{\rho}^t)$ and $\bar{\boldsymbol{\rho}}$ is the vector of maximum allowable prices. Equation (16b) ensures that the probability of aggregate load exceeding $P_{\max}$ is less than ϵ. The expectation in (16a) can be evaluated as

$$\begin{aligned} U^t(\boldsymbol{\rho}^t) &:= \mathbb{E}\left\{u_{\text{tot}}^t - \left[\alpha\left(d_{\text{tot}}^t\right)^2 + \beta d_{\text{tot}}^t + \gamma\right] \middle| \boldsymbol{\rho}^t\right\} \\ &= \sum_{i=1}^{M} \left[\rho_i^t P_{\text{EV}} - \alpha\left(P_{\text{EV}}^2 + 2P_{\text{EV}} \sum_{j=1}^{M} \eta_j^t\right) - \beta P_{\text{EV}}\right] \\ &\quad \times p_{\hat{\boldsymbol{\theta}}^t}\left(b_i^t = 1 \middle| \boldsymbol{\rho}^t\right) \\ &\quad - \alpha \sum_{i=1}^{M} \sum_{\substack{j=1 \\ j\neq i}}^{M} P_{\text{EV}}^2 p_{\hat{\boldsymbol{\theta}}^t}\left(b_i^t = 1, b_j^t = 1 | \boldsymbol{\rho}^t\right) \\ &\quad + \sum_{i=1}^{M} \left(\rho_i^t - \beta\right)\eta_i^t - \alpha\left(\sum_{i=1}^{M} \eta_i^t\right)^2 - \gamma \end{aligned} \tag{17}$$

using the marginal probabilities $p_{\hat{\boldsymbol{\theta}}^t}(b_i^t = 1|\boldsymbol{\rho}^t)$ and $p_{\hat{\boldsymbol{\theta}}^t}(b_i^t = 1, b_j^t = 1|\boldsymbol{\rho}^t)$ obtained from the BP algorithm.

In order to obtain a tractable closed-form approximation of the risk constraint (16b), the central limit theorem is invoked, which holds for a sum of dependent random variables under appropriate mixing conditions [33]–[35]. Specifically, d_{tot}^t is approximated as Gaussian-distributed with mean and variance given as

$$\bar{\mu}^t(M) := \mathbb{E}\left\{d_{\text{tot}}^t | \boldsymbol{\rho}^t\right\} = \sum_{i=1}^{M} \left[p_{\hat{\boldsymbol{\theta}}^t}\left(b_i^t = 1 | \boldsymbol{\rho}^t\right) P_{\text{EV}} + \eta_i^t\right] \tag{18}$$

$$\begin{aligned} \left(\sigma^t(M)\right)^2 &:= \text{var}\{d_{\text{tot}}^t | \boldsymbol{\rho}^t\} \\ &= P_{\text{EV}}^2 \sum_{i=1}^{M} \left[p_{\hat{\boldsymbol{\theta}}^t}\left(b_i^t = 1 | \boldsymbol{\rho}^t\right)\right. \\ &\qquad + \sum_{\substack{j=1 \\ j\neq i}}^{M} p_{\hat{\boldsymbol{\theta}}^t}\left(b_i^t = 1, b_j^t = 1 | \boldsymbol{\rho}^t\right) \\ &\qquad \left. - \sum_{j=1}^{M} p_{\hat{\boldsymbol{\theta}}^t}(b_i^t = 1 | \boldsymbol{\rho}^t) p_{\hat{\boldsymbol{\theta}}^t}\left(b_j^t = 1 | \boldsymbol{\rho}^t\right)\right] \end{aligned} \tag{19}$$

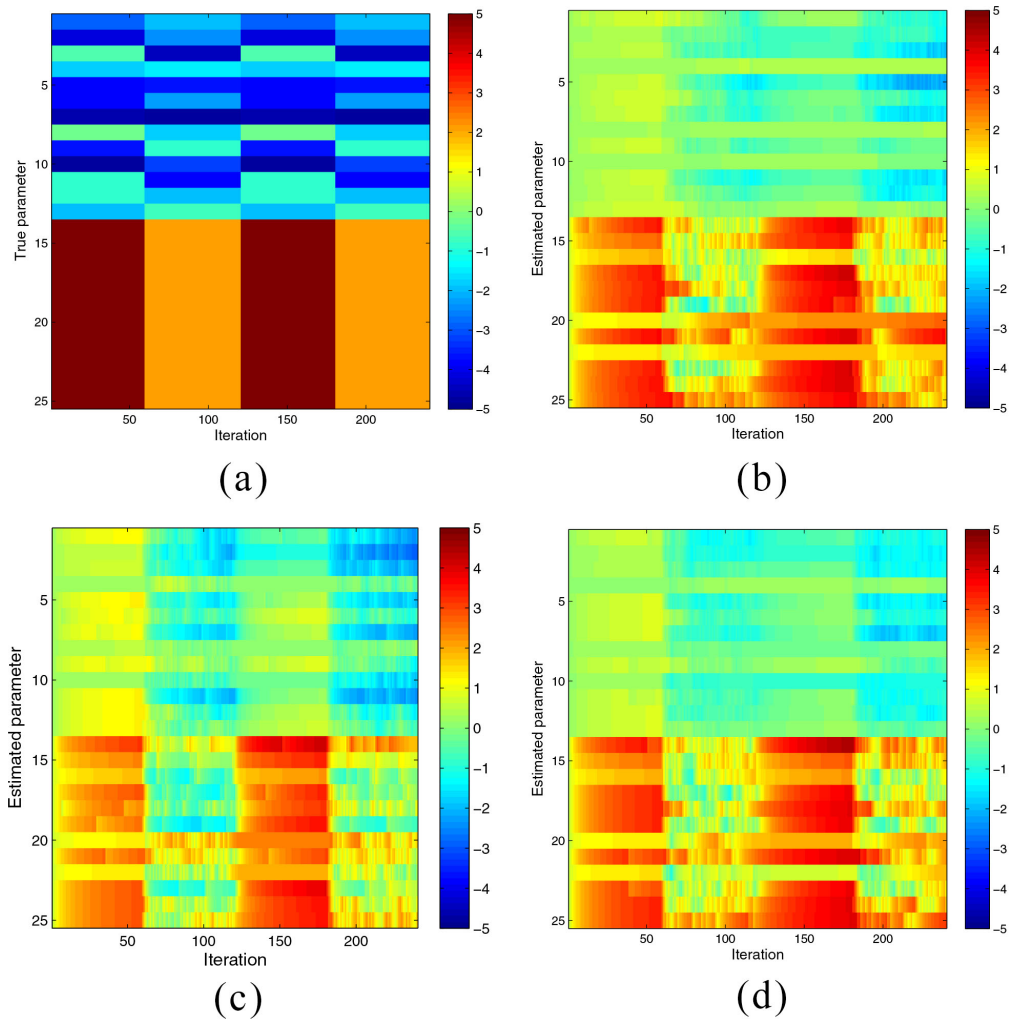

Fig. 2. True and estimated model parameters $\boldsymbol{\theta}^t$. (a) True parameters. (b) Random prices. (c) Constant prices. (d) ToU prices.

respectively. Based on this approximation, one can replace (16b) with

$$\bar{\mu}^t(M) - P_{\max} + \sigma^t(M) Q^{-1}(\epsilon) \leq 0 \tag{20}$$

where $Q(\cdot)$ is the standard Gaussian tail function. Thus, the optimization problem to solve is

$$\text{(P2)} \qquad \max_{\mathbf{0} \preceq \boldsymbol{\rho}^t \preceq \bar{\boldsymbol{\rho}}} U^t(\boldsymbol{\rho}^t) \text{ subject to (20).} \tag{21}$$

Since the conditional marginals are log-concave with respect to $\boldsymbol{\rho}^t$ [36], (P2) is not convex in general. In the next section, locally optimal solutions to (P2) are sought using the "fmincon" function in the MATLAB package.

Remark 1: Since the price setting is posed as a stochastic optimization problem, it can be tailored to incorporate any additional regulatory, socio-ethical, and operational constraints. For example, setting the prices equal for different consumers is possible through constraints like (27). One can perform zone-based pricing by setting prices equal within zones. Various regulatory constraints on the tarrifs as well as the grid operational constraints such as the optimal power-flow and the frequency regulation can also be accommodated as additional constraints, although this is beyond the scope of this paper. The bottom line is that while our focus is on incorporating consumer behavioral analytics into the pricing mechanism, the formulation is flexible enough to accommodate various deployment constraints.

V. Numerical Tests

The performance of the proposed algorithm was verified via numerical tests. Both fully simulated data and semi-real data were utilized.

A. Simulated Data

A set of 13 EV owners was considered, whose spatial dependencies were captured by graph G in Fig. 1. Given the true CRF parameters $\boldsymbol{\theta}^{*t}$, the charging decisions $\mathbf{b}^t$ were the samples from the CRF model in (1a)–(3), with $\boldsymbol{\rho}^t$ chosen as explained next. The values of $\boldsymbol{\theta}^{*t}$ were changed occasionally but otherwise were kept fixed over time; see Fig. 2(a), which depicts $\boldsymbol{\theta}^{*t}$. To test the tracking performance of the proposed method, three simple strategies for selecting $\boldsymbol{\rho}^t$ independent of estimated parameters are considered here: 1) constant prices; 2) time-of-use (ToU) prices; and 3) random prices. For the constant pricing setup, ρ_i^t was set to 1 for all consumers and

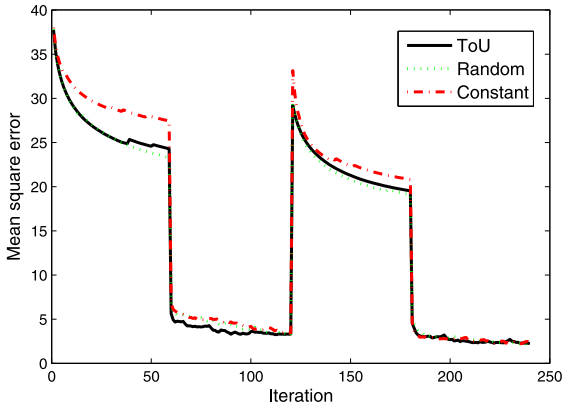

Fig. 3. Average squared prediction error for CRF parameters.

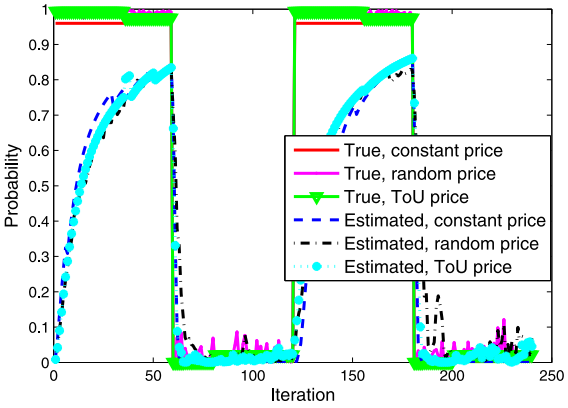

Fig. 4. Joint probability of consumer charging decisions.

held constant across time. For ToU pricing, the following was used:

$$\rho_i^t = \begin{cases} \$0.508 & 7 \text{ A.M.–2 P.M.} \\ \$0.880 & 2 \text{ P.M.–8 P.M.} \\ \$0.722 & 8 \text{ P.M.–11 P.M.} \\ \$0.508 & 11 \text{ P.M.–7 A.M.} \end{cases} \quad \forall i \in V. \tag{22}$$

In random pricing, the prices were randomly selected from a uniform distribution over $[0, 1]$. Prices were updated every 12 min, which corresponds to the duration of one time slot. A step size $\mu^t = 0.72$ was used. Fig. 2 shows true and estimated parameters under pricing strategies 1)–3). The y-axes of the subplots represent the parameter indices. The parameters indexed from 1 to 13 are the price dependency parameters $\{\theta_i^t\}_{i\in V}$, and the rest the spatial dependency $\{\theta_{i,j}\}_{(i,j)\in E}$.

Fig. 3 depicts the squared prediction error of the parameters, averaged over $M + N_e = 25$ parameters. For all price setting mechanisms, the errors tend to decrease as iterations progress, while sharp changes in the prediction error result whenever the parameter values are changed abruptly.

A comparison of $p_{\hat{\theta}^t}(\mathbf{b}^t_{\text{revealed}}|\boldsymbol{\rho}^t)$ with $p_{\boldsymbol{\theta}^{*t}}(\mathbf{b}^t_{\text{revealed}}|\boldsymbol{\rho}^t)$ per iteration is shown in Fig. 4. It can be seen that the joint probability of the charging decisions is tracked very well.

Once the joint probabilities $p(\mathbf{b}^t|\boldsymbol{\rho}^t)$ have been estimated, the expected value of the total load can be readily found as $\bar{P}^t_{\text{tot}} := P_{\text{EV}} \sum_{i=1}^{M} p_{\hat{\boldsymbol{\theta}}^t}(b_i^t = 1|\boldsymbol{\rho}^t)$. The predicted total loads are

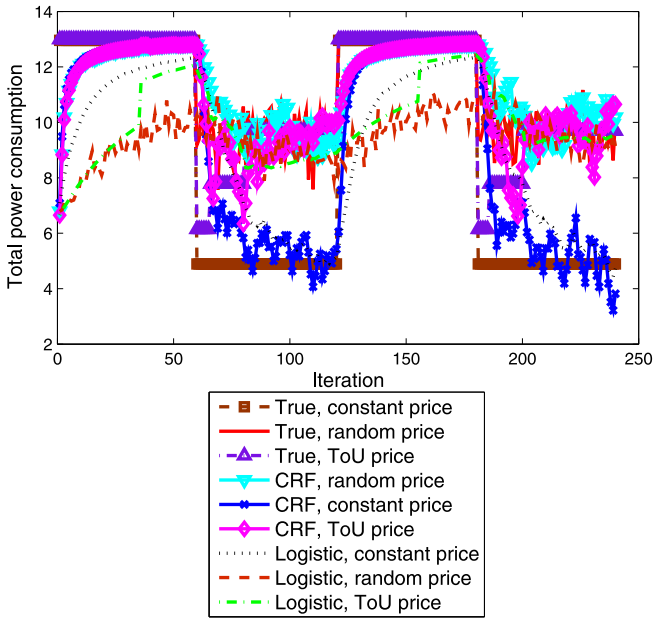

Fig. 5. Predicted total EV charging load $\bar{P}^t_{\text{tot}}$.

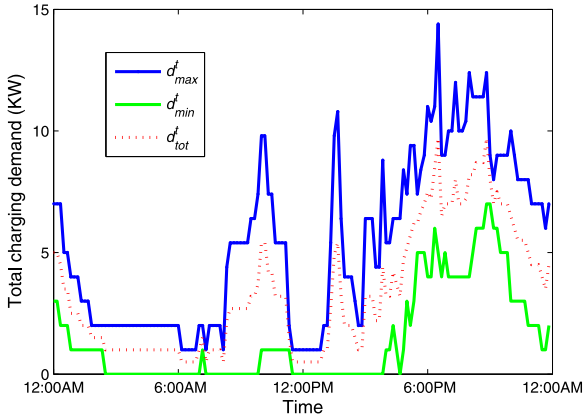

Fig. 6. Charging demand of 25 households [37].

depicted in Fig. 5, where the CRF-based estimates and the logistic regression-based ones are plotted together for comparison. The CRF-based algorithm achieves the performance gain by incorporating spatial dependencies.

B. Semi-Real Data

To validate the proposed methods in a more realistic setting, the experimental data of charging demand collected from 25 Northern California households in [37] were used in the tests. The project ran from August 2008 to April 2010, and the collected data have been aggregated to a single summary week. The charging power flow of EV, was assumed to be $P_{\text{EV}} = 1.4$ kW in all the experiments. Fig. 6 depicts the daily total demand data collected every 10 min with the price held equal at all times and for all consumers; that is, $\rho_i^t = 1$, $\forall i, t$. The three curves in Fig. 6 correspond to the highest demand $d^t_{\max}$ at each time t, the lowest demand $d^t_{\min}$, and their average

$$\bar{d}^t_{\text{tot}} := \frac{d^t_{\max} + d^t_{\min}}{2}. \tag{23}$$

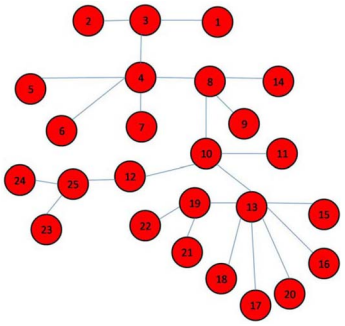

Fig. 7. Spatial dependency graph for semi-real data.

To evaluate the proposed model, data that capture consumers' charging behaviors in response to price changes are necessary. For this, a reasonable consumer behavioral model is concocted as delineated next, which is then fitted such that when the prices are held fixed at $\rho_i^t = 1$, the total demand curves as shown in Fig. 6 are obtained.

1) Consumer Behavior Model: A simple consumer behavior model is adopted, where consumer i charges when the price ρ_i^t is less than some threshold τ_i^t. That is, b_i^t is modeled as

$$b_i^t = \begin{cases} 1, & \text{if } \rho_i^t < \tau_i^t \\ 0, & \text{otherwise} \end{cases} \tag{24}$$

for $i \in V$ and $t = 1, 2, \ldots$. Note that $\tau_i^t < 0$ can model the case where the EV i is fully charged.

Let $\boldsymbol{\tau}^t := [\tau_1^t, \ldots, \tau_M^t]$ and $P_{\text{tot}}^t := P_{\text{EV}} \sum_{i=1}^M b_i^t$. In order to capture the spatial dependency of charging behaviors, $\boldsymbol{\tau}^t$ is sampled from a Gaussian distribution with mean $\boldsymbol{\mu}^t$ and covariance $\boldsymbol{\Sigma}^t$, where $\boldsymbol{\Sigma}^t$ encodes the dependency graph G shown in Fig. 7, via

$$\left[\boldsymbol{\Sigma}^t\right]_{ij} = \begin{cases} r_{ij}^t, & \text{if } (i,j) \in E \\ r_{ii}^t, & \text{if } i = j \\ 0, & \text{otherwise} \end{cases} \tag{25}$$

with $r_{ij}^t > 0$ for $i, j \in V$. Using again the central limit theorem for dependent random variables, P_{tot}^t can be approximated to follow a Gaussian distribution with mean μ_S^t and variance $(\sigma_S^t)^2$. To fit the model to the real data when $\rho_i^t = 1$ for all i, t, the positive definiteness of $\boldsymbol{\Sigma}^t$, as well as the following relations are used to determine parameters $\{r_{ij}^t\}$:

$$\mu_S^t = \bar{d}_{\text{tot}}^t, \quad \sigma_S^t = \frac{d_{\max}^t - d_{\min}^t}{4}. \tag{26}$$

Fig. 8 shows the result of the fitting. The dotted curve shows the total charging demand obtained through the model in (24) and (25) averaged over 28 realizations, and the solid curve represents $\bar{d}_{\text{tot}}^t$ due to the real data. It can be seen that real charging demand matches well with the value obtained from the proposed behavior model.

2) Online Model Parameter Learning: The performance of the proposed online learning algorithm was tested using the semi-real data. Fig. 9 shows the average predicted total charging demands $\bar{P}_{\text{tot}}^t$ (averaged over 28 realizations) using the CRF and logistic regression models, based on the input generated from the model in (24) and (25) under constant pricing.

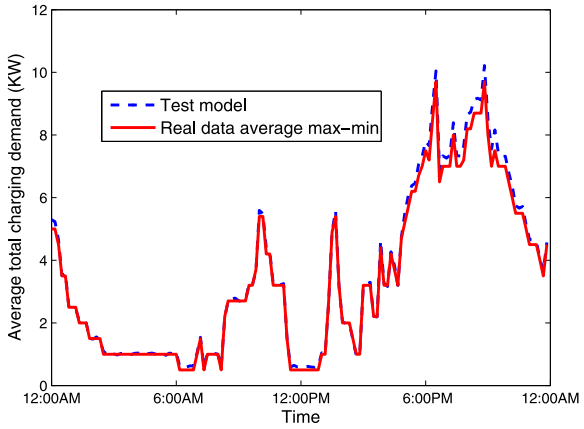

Fig. 8. Real and simulated total charging demands.

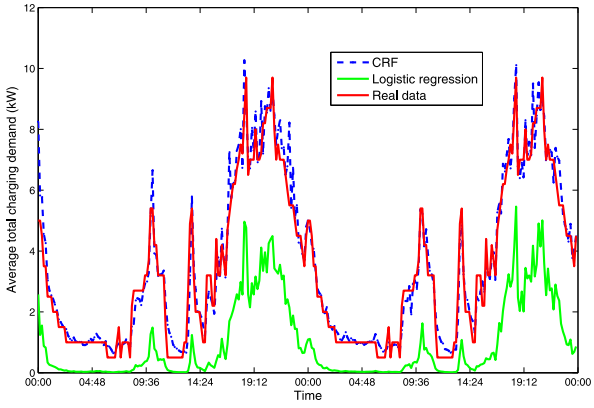

Fig. 9. Predicted average total charging demands.

The model parameters $\{\boldsymbol{\theta}^t\}$ were tracked using the algorithm in Table II. It can be seen that the prediction is very accurate when the CRF model is used. However, similar to the case of simulated data, the logistic regression model produces predictions that are quite off from the true values. Note that the initial performance degradation seen in the CRF curve is due to the transient effect in tracking, which depends on the initial value of $\boldsymbol{\theta}^t$.

3) Real-Time Pricing: Finally, the real-time price setting formulation discussed in Section IV is tested. Here, $\epsilon = 0.001$ and $P_{\max}$ was set to 5 kW, and $\bar{\boldsymbol{\rho}} = [2, 2, \ldots, 2]$ was used. The case of zero base load was considered; i.e., $\eta_i^t = 0$ for all i and t. The generator parameters were chosen to be $\alpha = 0.15$, $\beta = 0.4$, and $\gamma = 0$. In addition to the most general price setting formulation (P2), a special case of setting the prices equal to all consumers was also considered. That is

$$\rho_1 = \rho_2 = \cdots = \rho_M^t = \rho^t \tag{27}$$

was enforced in (P2) at each time t. Fig. 10 depicts the net profit and the total EV charging load under real-time pricing. The dash-dot curve in Fig. 10(a) is the net profit obtained from model (24) when prices are set through (P2), and the dashed curve corresponds to the case of equal pricing under (27). For comparison, the net profit under fixed pricing at $\rho_i^t = 1$ for all i and t as in the real data is also plotted in the solid curve. From Fig. 10(a), it can be observed that the profit is generally much improved by employing real-time pricing, compared to

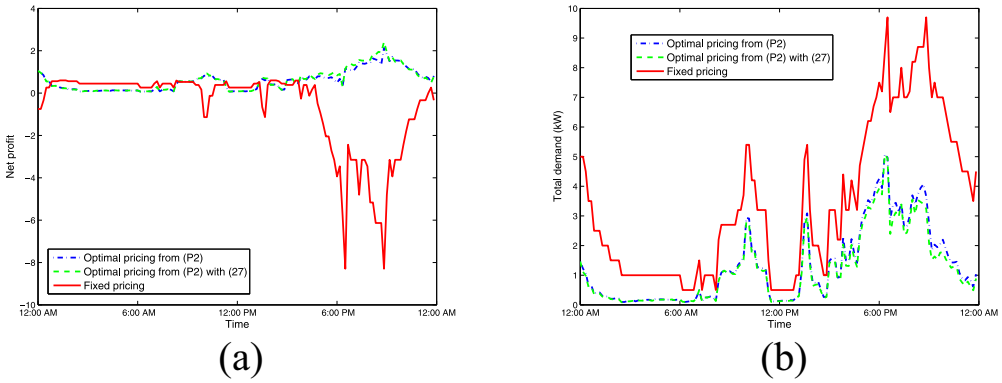

Fig. 10. Net profit and total charging demand under real-time pricing. (a) Net profit. (b) Total charging demand.

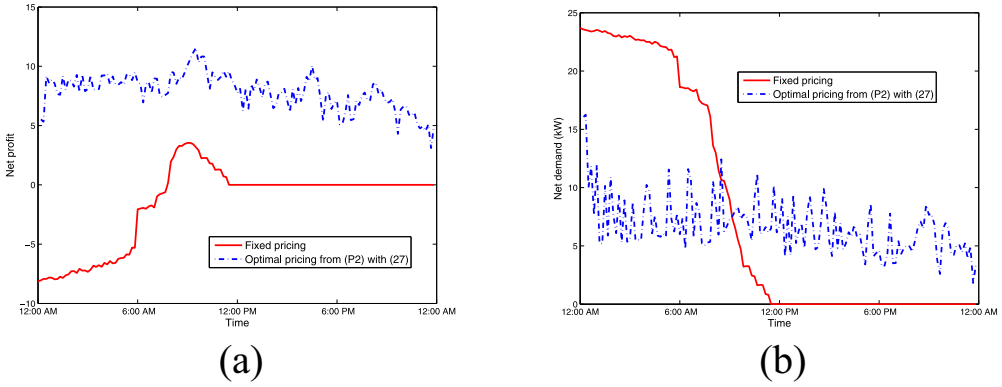

Fig. 12. Net profit and total charging demand with (28). (a) Net profit. (b) Total charging demand.

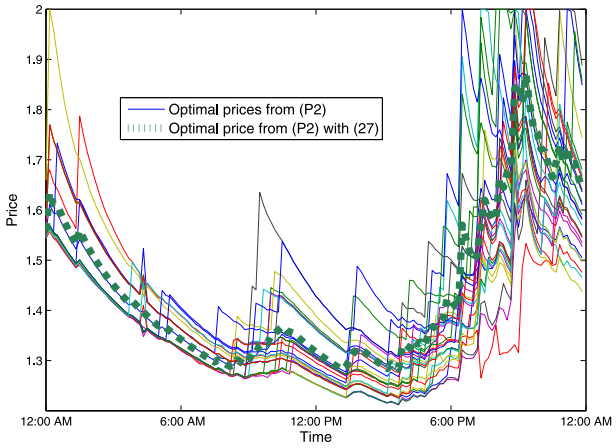

Fig. 11. Real-time prices.

the curve for which fixed pricing was used. However, since the tracking is not perfect, and the solutions to (P2) may suffer from local optima, the profit does not always stay at the optimum. The load curve in Fig. 10(b) clearly shows that the demand is flattened by real-time pricing, as the economically favorable operating point is tracked. Interestingly, it is noted that adopting identical prices across customers incurs almost no performance loss.

Fig. 11 depicts $\{\rho_i^{*t}\}$ for the individual customers $i \in V$ from solving (P2) in the solid curves, as well as ρ^t from (P2) with the additional constraint (27) in the thick dashed curve. The initial peaks are due to the constraint (16b) being tight with $P_{\max}$ set to 5 kW.

4) Test With Charging Capacity and Deadline Constraints: Here, the proposed real-time pricing algorithm is tested with a slightly different consumer behavior model, where the consumers have total energy target for EV charging as well as the charging deadline. As more energy is left to be charged and the deadline is approached, the consumer is modeled to behave less elastically.

To capture this, let $\mathcal{E}_i$ and $\mathcal{D}_i$ denote the energy left to be charged at time t and the time left until the deadline for the ith consumer, respectively. We still use the behavior model in (24), but now τ_i^t is determined as

$$\tau_i^t = \begin{cases} \zeta_i \mathcal{E}_i^t / \mathcal{D}_i^t + \nu_i^t + |\lambda^t|, & \text{if } \mathcal{E}_i^t > 0 \text{ and } \mathcal{D}_i^t > 0 \\ 0, & \text{otherwise} \end{cases} \tag{28}$$

where $\boldsymbol{\nu}^t := [\nu_1^t, ..., \nu_M^t]$ is a zero-mean Gaussian noise vector with its covariance matrix obtained as (25), $\lambda^t := \min_i \nu_i^t$ introduced to make sure $\tau_i \geq 0$, and ζ_i controls the sensitivity to the charging constraints. $P_{\max}$ was set to 15 kW, and $\alpha = 0.05$ and $\beta = 0.1$ were used. ζ, $\mathcal{E}_i^0$, and $\mathcal{D}_i^0$ were uniformly sampled from [0, 1], [6, 10] kWh, and [6, 24] h, respectively. The rest of the parameters remained the same as the previous experiment.

Fig. 12(a) shows that the net profit from solving (P2) with (27) is considerably higher than the profit with the fixed pricing strategy. From Fig. 12(b), it can be seen that through real-time pricing, the net demand is considerably flattened,

whereas the demand with the fixed pricing suffers from a large peak demand due to simultaneous charging of the EVs.

VI. Conclusion

An algorithm to track the elasticity of individual EV charging loads was developed. Such information is essential for setting the electricity prices in real time to coordinate EV charging. The probabilities with which individual EV consumers charge their vehicles when presented with real-time prices were obtained based on a CRF model, in which the spatial dependency of the customers' behavior was captured. Without explicit models for temporal dynamics, an online learning algorithm to estimate the CRF parameters was derived in the framework of online convex optimization. The CRF model was then applied as an input to an stochastic profit maximization problem for real-time price setting. The performance of the proposed algorithms was corroborated using simulated and semi-real data.

Appendix

Derivation of (8) and (9)

Differentiating the $-\log$ of the pdf in (1) yields

$$\frac{\partial \ell^t}{\partial \theta_i^t} = \frac{\partial \log Z(\boldsymbol{\rho}^t)}{\partial \theta_i^t} - b_i^t \rho_i^t, \qquad \forall i \in V$$
$$\frac{\partial \ell^t}{\partial \theta_{i,j}^t} = \frac{\partial \log Z(\boldsymbol{\rho}^t)}{\partial \theta_{i,j}^t} - b_i^t b_j^t, \qquad \forall (i,j) \in E$$

where after substituting $Z(\boldsymbol{\rho}^t)$ from (1b), it follows:

$$\frac{\partial \log Z(\boldsymbol{\rho}^t)}{\partial \theta_i^t} = \frac{1}{Z(\boldsymbol{\rho}^t)} \sum_{\mathbf{b}^t} b_i^t \rho_i^t \exp\left(\sum_{i=1}^N \theta_i^t b_i^t \rho_i^t + \sum_{i,j \in E} \theta_{i,j}^t b_i^t b_j^t \right)$$
$$= \mathbb{E}\left\{ b_i^t \rho_i^t | \boldsymbol{\rho}^t \right\}, \qquad \forall i \in V$$
$$\frac{\partial \log Z(\boldsymbol{\rho}^t)}{\partial \theta_{i,j}^t} = \frac{1}{Z(\boldsymbol{\rho}^t)} \sum_{\mathbf{b}^t} b_i^t b_j^t \exp\left(\sum_{i=1}^N \theta_i^t b_i^t b_j^t + \sum_{i,j \in E} \theta_{i,j}^t b_i^t \rho_i^t \right)$$
$$= \mathbb{E}\left\{ b_i^t b_j^t | \boldsymbol{\rho}^t \right\}, \qquad \forall (i,j) \in E$$

thus completing the proof.

Proof of Proposition 1

The regret of online gradient descent algorithm for convex loss function, $\ell^t(\boldsymbol{\theta}^t)$, is bounded by [17]

$$R_T(\boldsymbol{\theta}) := \sum_{t=1}^T \ell^t(\boldsymbol{\theta}^t) - \sum_{t=1}^T \ell^t(\boldsymbol{\theta}) \leq \frac{1}{2\mu_t} \|\boldsymbol{\theta}\|^2 + \mu_t \sum_{t=1}^T \left\| \nabla \ell^t \right\|^2. \tag{29}$$

Since $b_i^t \in \{0,1\}$, $0 \leq p_{\boldsymbol{\theta}^t}(b_i^t = 1 | \boldsymbol{\rho}^t) \leq 1$, and $0 \leq p_{\boldsymbol{\theta}^t}(b_i^t = 1, b_j^t = 1 | \boldsymbol{\rho}^t) \leq 1$, it follows from (8) and (9) that the gradients are bounded as:

$$-\rho_i^t \leq \frac{\partial \ell^t}{\partial \theta_i^t} \leq \rho_i^t \qquad \forall i \in V \tag{30a}$$
$$-1 \leq \frac{\partial \ell^t}{\partial \theta_{i,j}^t} \leq 1 \qquad \forall (i,j) \in E. \tag{30b}$$

Upon assuming that the price is bounded, i.e., $|\rho_i^t| \leq \rho_0$ for all t, $i \in V$, it follows that $\|\boldsymbol{\rho}^t\|^2 \leq M\rho_0^2$. Letting $N_e := |E|$ denote the number of edges in E, it then holds that $\|\nabla \ell^t\|^2 \leq M\rho_0^2 + N_e$. If $\max\{|\theta_i^t|, |\theta_{i,j}^t|\} \leq \theta_0$ and we further choose $\mu_t = \theta_0 / \sqrt{(2(M\rho_0^2 + N_e)T}$, the regret boils down to

$$R_T \leq \theta_0 \sqrt{2(M\rho_0^2 + N_e)T} = O(\sqrt{T}). \tag{31}$$

References

[1] International Energy Agency. (2011). *Technology Roadmap Electric and Plug-In Hybrid Electric Vehicles*. [Online]. Available: http://www.iea.org/publications/freepublications/publication/EV_PHEV_Roadmap.pdf

[2] K. Clement-Nyns, E. Haesen, and J. Driesen, "The impact of charging plug-in hybrid electric vehicles on a residential distribution grid," *IEEE Trans. Power Syst.*, vol. 25, no. 1, pp. 371–380, Jan. 2010.

[3] A. Putrus, P. Suwanapingkarl, D. Johnston, E. C. Bentley, and M. Narayana, "Impact of electric vehicles on power distribution network," in *Proc. IEEE Vehicle Power Propul. Conf.*, Dearborn, MI, USA, Sep. 2009, pp. 827–831.

[4] R. Liu, L. Dow, and E. Liu, "A survey of PEV impacts on electric utilities," in *Proc. Innov. Smart Grid Technol.*, Anaheim, CA, USA, Jan. 2011, pp. 1–8.

[5] K. Parks, P. Denholm, and T. Markel, "Costs and emissions associated with plug-in hybrid electric vehicle charging in the XCEL energy Colorado service territory," Nat. Renewable Energy Lab., Golden, CO, USA, Tech. Rep. NREL/TP-640-41410, 2007.

[6] Z. Ma, D. Callaway, and I. Hiskens, "Decentralized charging control of large populations of plug-in electric vehicles," *IEEE Trans. Control Syst. Technol.*, vol. 21, no. 1, pp. 67–78, Nov. 2013.

[7] S. Sojoudi and S. H. Low, "Optimal charging of plug-in hybrid electric vehicles in smart grids," in *Proc. IEEE Power Energy Soc. Gen. Meeting*, Detroit, MI, USA, Jul. 2011, pp. 1–6.

[8] L. Gan, U. Topcu, and S. Low, "Optimal decentralized protocol for electric vehicle charging," *IEEE Trans. Power Syst.*, vol. 28, no. 2, pp. 940–951, May 2013.

[9] E. Sortomme, M. M. Hindi, S. D. J. MacPherson, and S. S. Venkata, "Coordinated charging of plug-in hybrid electric vehicles to minimize distribution system losses," *IEEE Trans. Smart Grid*, vol. 2, no. 1, pp. 198–205, Mar. 2011.

[10] L. Gan, A. Wierman, U. Topcu, N. Chen, and S. Low, "Real-time deferrable load control: Handling the uncertainties of renewable generation," in *Proc. ACM Int. Conf. Future Energy Syst.*, Berkeley, CA, USA, May 2013, pp. 113–124.

[11] L. Gan, U. Topcu, and S. H. Low, "Stochastic distributed protocol for electric vehicle charging with discrete charging rate," in *Proc. IEEE Power Energy Soc. Gen. Meeting*, San Diego, CA, USA, 2012, pp. 1–8.

[12] S. Deilami, A. Masoum, P. Moses, and M. Masoum, "Real-time coordination of plug-in electric vehicle charging in smart grids to minimize power losses and improve voltage profile," *IEEE Trans. Smart Grid*, vol. 2, no. 3, pp. 456–467, May 2011.

[13] J. Soares, H. Morais, T. Sousa, Z. Vale, and P. Faria, "Day-ahead resource scheduling including demand response for electric vehicles," *IEEE Trans. Smart Grid*, vol. 4, no. 1, pp. 596–605, Mar. 2013.

[14] V. Gomez, M. Chertkov, S. Backhaus, and H. Kappen, "Learning price-elasticity of smart consumers in power distribution systems," in *Proc. IEEE Int. Conf. Smart Grid Commun.*, Tainan City, Taiwan, Nov. 2012, pp. 647–652.

[15] C. Ibars, M. Navarro, and L. Giupponi, "Distributed demand management in smart grid with a congestion game," in *Proc. IEEE Int. Conf. Smart Grid Commun.*, Gaithersburg, MD, USA, Oct. 2010, pp. 495–500.

[16] J. Lafferty, A. McCallum, and F. Pereira, "Conditional random fields: Probabilistic models for segmenting and labeling sequence data," in *Proc. Int. Conf. Mach. Learning*, Williamstown, MA, USA, Jun./Jul. 2001, pp. 282–289.

[17] S. Shalev-Shwartz, "Online learning and online convex optimization," *Found. Trends Mach. Learn.*, vol. 4, no. 2, pp. 107–194, 2011.

[18] C. Sutton and A. McCallum. (Nov. 2010). "An introduction to conditional random fields," pp. 1–90. [Online]. Available: http://arxiv.org/abs/1011.4088v1

[19] W. Tushar, W. Saad, H. V. Poor, and D. Smith, "Economics of electric vehicle charging: A game theoretic approach," *IEEE Trans. Smart Grid*, vol. 3, no. 4, pp. 1767–1779, Dec. 2012.

[20] C. Wu, H. Mohsenian-Rad, and J. Huang, "Vehicle-to-aggregator interaction game," *IEEE Trans. Smart Grid*, vol. 3, no. 1, pp. 434–442, Mar. 2012.
[21] Y. Wang, W. Saad, Z. Han, H. V. Poor, and T. Baar, "A game-theoretic approach to energy trading in the smart grid," *IEEE Trans. Smart Grid*, vol. 5, no. 3, pp. 1439–1450, May 2014.
[22] R. Yu, W. Yang, and S. Rahardja, "A statistical demand-price model with its application in optimal real-time price," *IEEE Trans. Smart Grid*, vol. 3, no. 4, pp. 1734–1742, Dec. 2012.
[23] P. Tarasak, "Optimal real-time pricing under load uncertainty based on utility maximization for smart grid," in *Proc. IEEE Int. Conf. Smart Grid Commun.*, Brussels, Belgium, Oct. 2011, pp. 321–326.
[24] N. Y. Soltani, S.-J. Kim, and G. B. Giannakis, "Online learning of load elasticity for electric vehicle charging," in *Proc. IEEE 5th Int. Workshop Comput. Adv. Multi-Sensor Adapt. Process. (CAMSAP)*, St. Martin, The Netherlands, Dec. 2013, pp. 436–439.
[25] M. J. Wainwright and M. I. Jordan, "Graphical models, exponential families, and variational inference," *Found. Trends Mach. Learn.*, vol. 1, nos. 1–2, pp. 1–305, 2008.
[26] E. Hazan, A. Agarwal, and S. Kayle, "Logarithmic regret algorithms for online convex optimization," *J. Mach. Learn.*, vol. 69, no. 3, pp. 169–192, Dec. 2007.
[27] M. Zinkevich, "Online convex programming and generalized infinitesimal gradient ascent," in *Proc. 20th Int. Conf. Mach. Learn.*, Washington, DC, USA, Aug. 2003, pp. 928–936.
[28] T. Hastie, R. Tibshirani, and J. Friedman, *The Elements of Statistical Learning*, 2nd ed. New York, NY, USA: Springer, 2009.
[29] M. Raginsky, R. F. Marcia, S. Jorge, and R. Willett, "Sequential probability assignment via online convex programming using exponential families," in *Proc. IEEE Int. Symp. Inf. Theory*, Seoul, Korea, Jun./Jul. 2009, pp. 1338–1342.
[30] N. Srebro, K. Sridharan, and A. Tewari, "On the universality of online mirror descent," in *Proc. Adv. Neural Inf. Process. Syst.*, Granada, Spain, Dec. 2011, pp. 2645–2653.
[31] J. S. Yedidia, W. T. Freeman, and Y. Weiss, "Bethe free energy, Kikuchi approximations, and belief propagation algorithms," Mitsubishi Elect. Res. Lab., Cambridge, MA, USA, Tech. Rep. TR-2001-16, May 2001.
[32] H. Kushner and G. Yin, *Stochastic Approximation Algorithms and Applications*, 2nd ed. New York, NY, USA: Springer, 2003.
[33] P. Billingsley, *Probability Measure*, 3rd ed. Hoboken, NJ, USA: Wiley, 1995.
[34] R. C. Bradley, "Basic properties of strong mixing conditions. A survey and some open questions," *Probab. Surveys*, vol. 2, pp. 107–144, Apr. 2005.
[35] N. Ross, "Fundamentals of Stein's method," *Probab. Surveys*, vol. 8, pp. 210–293, Sep. 2011.
[36] M. Bagnoli and T. Bergstrom, "Log-concave probability and its applications," *Econ. Theory*, vol. 26, pp. 445–469, Aug. 2005.
[37] J. Davies and K. Kurani, "Moving from assumption to observation: Implications for energy and emissions impacts plug-in hybrid electric vehicles," *Energy Policy*, vol. 62, pp. 550–560, Nov. 2013.

Nasim Yahya Soltani (S'13) received the B.Sc. degree in electrical and computer engineering from the University of Tehran, Tehran, Iran, in 2003, and the M.Sc. and Ph.D. degrees in electrical engineering from the Iran University of Science and Technology, Tehran, and the University of Minnesota, Minneapolis, MN, USA, in 2006 and 2014, respectively.

She is currently a Research Associate with the Digital Technology Center, University of Minnesota. Her current research interests include statistical signal processing, machine learning, optimization, network science, and big data analytics with their applications to power grid and wireless communications.

Seung-Jun Kim (SM'12) received the B.S. and M.S. degrees from Seoul National University, Seoul, Korea, in 1996 and 1998, respectively, and the Ph.D. degree from the University of California, Santa Barbara, CA, USA, in 2005, all in electrical engineering.

From 2005 to 2008, he was with NEC Laboratories America, Princeton, NJ, USA, as a Research Staff Member. From 2008 to 2014, he was with the Digital Technology Center, and the Department of Electrical and Computer Engineering, University of Minnesota, Minneapolis, MN, USA, where his final title was Research Associate Professor. Since 2014, he has been with the Department of Computer Science and Electrical Engineering, University of Maryland, Baltimore, MD, USA, as an Assistant Professor. His current research interests include statistical signal processing, optimization, and machine learning, with applications to wireless communication and networking, and future power systems.

Georgios B. Giannakis (F'97) received the Diploma degree in electrical engineering from the National Technical University of Athens, Athens, Greece, in 1981, and the M.Sc. degrees in electrical engineering and mathematics, and the Ph.D. degree in electrical engineering from the University of Southern California (USC), Los Angeles, CA, USA, in 1983, 1986, and 1986, respectively.

From 1982 to 1986, he was with USC. Since 1999, he has been a Professor with the University of Minnesota, Minneapolis, MN, USA, where he is currently an ADC Chair in wireless telecommunications with the Electrical and Computer Engineering Department, and serves as a Director of the Digital Technology Center. His current research interests include communications, networking, statistical signal processing, sparsity and big data analytics, wireless cognitive radios, mobile *ad hoc* networks, renewable energy, power grid, gene-regulatory, and social networks. He has published over 370 journal papers, 630 conference papers, 21 book chapters, two edited books, and two research monographs (h-index 110), and holds 23 patents.

Prof. Giannakis was the co-recipient of eight best paper awards from the IEEE Signal Processing (SP) and Communications Societies, including the G. Marconi Prize Paper Award in Wireless Communications. He was also the recipient of the Technical Achievement Award from the SP Society in 2000, European Association for Signal Processing (EURASIP) in 2005, a Young Faculty Teaching Award, the G. W. Taylor Award for Distinguished Research from the University of Minnesota, and the IEEE Fourier Technical Field Award in 2014. He is a Fellow of EURASIP, and has served the IEEE in several roles, including that of a Distinguished Lecturer for the IEEE-SP Society.